DEUTERIUM-TRITIUM TFTR PLASMAS WITH HIGH INTERNAL INDUCTANCE*

S. A. SABBAGH[1†], E. D. FREDRICKSON[2], D. K. MANSFIELD[2], M. G. BELL[2], S. H. BATHA[3], R. E. BELL[2], R. V. BUDNY[2], C. E. BUSH[2], Z. CHANG[2], R. J. HAWRYLUK[2], D. W. JOHNSON[2], F. LEVINTON[3], J. MANICKAM[2], K. M. McGUIRE[2], D. MUELLER[2], F. PAOLETTI[1†], H. K. PARK[2], A. T. RAMSEY[2], C. H. SKINNER[2], E. J. SYNAKOWSKI[2], H. TAKAHASHI[2], G. TAYLOR[2], L. ZAKHAROV[2], M.C. ZARNSTORFF[2]

[1] Department of Applied Physics,
Columbia University,
New York, NY

[2] Princeton Plasma Physics Laboratory,
Princeton, NJ

[3] Fusion Physics and Technology, Inc.,
Torrance, CA

United States of America

Abstract

DEUTERIUM-TRITIUM TFTR PLASMAS WITH HIGH INTERNAL INDUCTANCE

Deuterium-tritium plasmas with increased plasma internal inductance, l_i, have been produced in TFTR to investigate stability limits at high l_i, I_p, and B_0, and to assess fusion power production in these plasmas. A novel technique of plasma initiation at low edge safety factor, q_a, has allowed operation at I_p up to 2.3 MA and l_i up to 1.5. These plasmas exhibit larger sawtooth inversion radii than plasmas with lower l_i at the same I_p. The sawteeth are stabilized at sufficiently large injected neutral beam heating power, P_b, consistent with a model of ω^*-stabilization. The stability limit due to disruption is consistent with a scaling of the maximum $\beta_N \equiv 10^8 <\beta_t> aB_0 / I_p$ being proportional to l_i. Increased energy confinement, attained by lithium conditioning of the limiter, has exceeded that of supershot plasmas at heating power levels above 30 MW. Fusion powers of up to 8.7 MW have been generated in these plasmas. At the maximum attempted I_p and B_0, the plasmas are no longer limited by gross plasma instability, but rather by limiter power handling. Plasmas with reversed central shear and increased l_i due to increased edge magnetic shear have also been created. The stability limit for these plasmas also exhibits an increase in the maximum β_N with increased l_i.

---

*Supported by US DoE Contracts DE-FG02-89ER53297, DE-AC02-76-CH03073, and DE-FG02-90ER54084.

†Present address: Plasma Physics Laboratory, Princeton University, P.O. Box 451, Princeton, NJ 08543, USA.

I. Introduction

Plasma instability driven by the plasma pressure is presently the most restrictive constraint on plasma performance in large tokamaks [1,2]. Understanding the dependence of the beta limit on plasma equilibrium parameters is therefore crucial to improving fusion power production in tokamak plasmas. Experiments in several machines including DIII-D [3,4], JT-60U [5], and TFTR [6] have shown that increasing the peakedness of the equilibrium current profile (i.e., increasing internal inductance, l_i) can lead to improvements in the normalized beta, $\beta_N \equiv 10^8 <\beta_t> aB_0 / I_p$, attainable in these machines. Here, a is the minor radius and B_0 is the toroidal magnetic field at the geometric center. This result agrees with ideal MHD stability calculations [7,8] that show a linear increase of the β_N limit with increasing l_i for equilibrium pressure profiles that are not excessively peaked.

A demonstration of increased plasma stability at maximum absolute parameters is a logical continuation of these experiments. The fusion power output, P_f, in high temperature tokamak plasmas heated by neutral beam injection scales approximately as the square of the plasma stored energy, W_{tot} [9].Therefore, if the maximum achievable normalized beta, β_{Nmax}, increases linearly with l_i, an increase in the maximum P_f can be obtained by increasing the product of l_i I_p B_0.

Technical aspects of generating the high l_i plasma in previous experiments, including TFTR [10], had limited operation to reduced I_p. Recently, deuterium-tritium plasmas with increased internal inductance have been produced in TFTR with monotonic q profiles at high I_p. A novel approach has been developed to create plasmas with both high $l_i \leq 1.5$ and high I_p = 2.0 - 2.3 MA with B_0 = 4.8 - 5.6 T ($q^* \equiv 5(a^2 B_0 / R_p I_p(\mathrm{MA}))(1+\kappa^2)/2$ = 3.4 - 3.6) to investigate beta limit physics at increased l_i I_p B_0 product, as well as to develop a test-bed for alpha physics studies at high fusion power.

Increasing the gross stability of plasmas with reversed magnetic field shear in the plasma core [11] has also been investigated in high poloidal β D-T plasmas with I_p = 0.8 - 1.0 MA and increased l_i created by rapidly decreasing I_p. We find that β_{Nmax} is also increased as l_i is increased in these plasmas.

The peak D-T fusion power output as a function of I_p for the recent high l_i plasmas created with $I_p \geq 2$ MA, as well as for supershots, reversed shear [11], weak shear plasmas [12], and previously reported high β_p, high l_i plasmas utilizing a rapid decrease in I_p to produce increased l_i [10] is shown in Fig. 1. Fusion powers of up to 8.7 MW have been generated in high l_i plasmas. The fusion power output and stored energy of the recent high l_i D-T plasmas at I_p = 2.3 MA and B_0 = 5.6T are presently not limited by plasma instability. Instead, they are limited by the occurrence of large density influxes from the limiter which occur at $W_{tot} \geq 6$ MJ and $P_b \geq 33$ MW. These "density bloom" events rapidly decrease τ_E. If this limiter power handling constraint could be removed, the increased stability margin of the high l_i plasmas should allow fusion power production in excess of 14 MW at the l_i I_p B_0 product already produced. The P_f for a given W_{tot} is also greater in high l_i I_p plasmas, exceeding 10% of the power normally generated by lower l_i supershots.

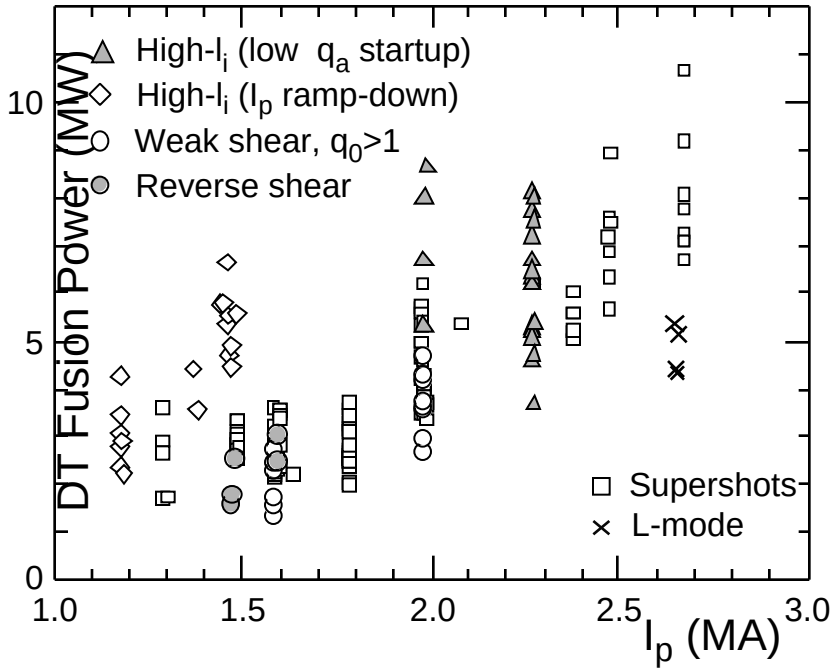

Figure 1 Fusion power output vs. I_p *for several TFTR operational regimes.*

II. Generation of high l_i plasma at high current

Details of the technique used to produce TFTR plasmas at both high l_i and high I_p are shown in Fig. 2. A peaked current profile was produced by initiating a deuterium ohmic plasma on the outer RF limiter with reduced minor radius, a_p = 0.46 m (about 53% of the final minor radius), and q_a = 2.3. The discharge was subsequently moved to the inner belt limiter (plasma major radius, R_p = 2.3 m), and I_p raised to 2.4 MA. This configuration formed the core of the subsequent high l_i plasma, which was created by expanding the minor radius to 0.87 m in 100 ms. Neutral beam injection power, P_b, up to 36 MW was used to heat the plasma. In this case, 70% of P_b is supplied by tritium neutral beams.

Several variants of this plasma growth scheme have been used to minimize MHD activity while retaining the high l_i I_p product by modifying the plasma growth evolution and using mild decreases in I_p. Also, q_a was sometimes raised to an intermediate value of 3.3 to allow injection of Li pellets without disruption. Pellet injection during this phase increases τ_E during NBI. Such a variation is indicated by the dashed trace in Fig. 2(a-c). Both the increase in l_i and l_i I_p generated in an equivalent ohmic plasma are shown in Fig 2(d-e). A typical value of l_i reached in supershot plasmas is shown for reference. In high l_i plasmas, l_i and l_i I_p have reached peak values of 1.5 and 3.4 MA respectively. Additional details of the plasma growth, and increased τ_E through lithium conditioning can be found in the papers of Fredrickson *et al.* [13], and Mansfield *et al.* [14].

Fusion power, plasma stored energy, and line-integrated edge density are shown in Fig. 2(f-g). A density bloom occurs in the plasma shortly after 4 s which reduces both the stored energy and fusion power output. The density evolution of a plasma which does not have a bloom is shown for comparison. The P_f and W_{tot} typically decrease after the edge density increases sharply. Central electron and ion temperatures of 8.3 keV and 42 keV, respectively, with

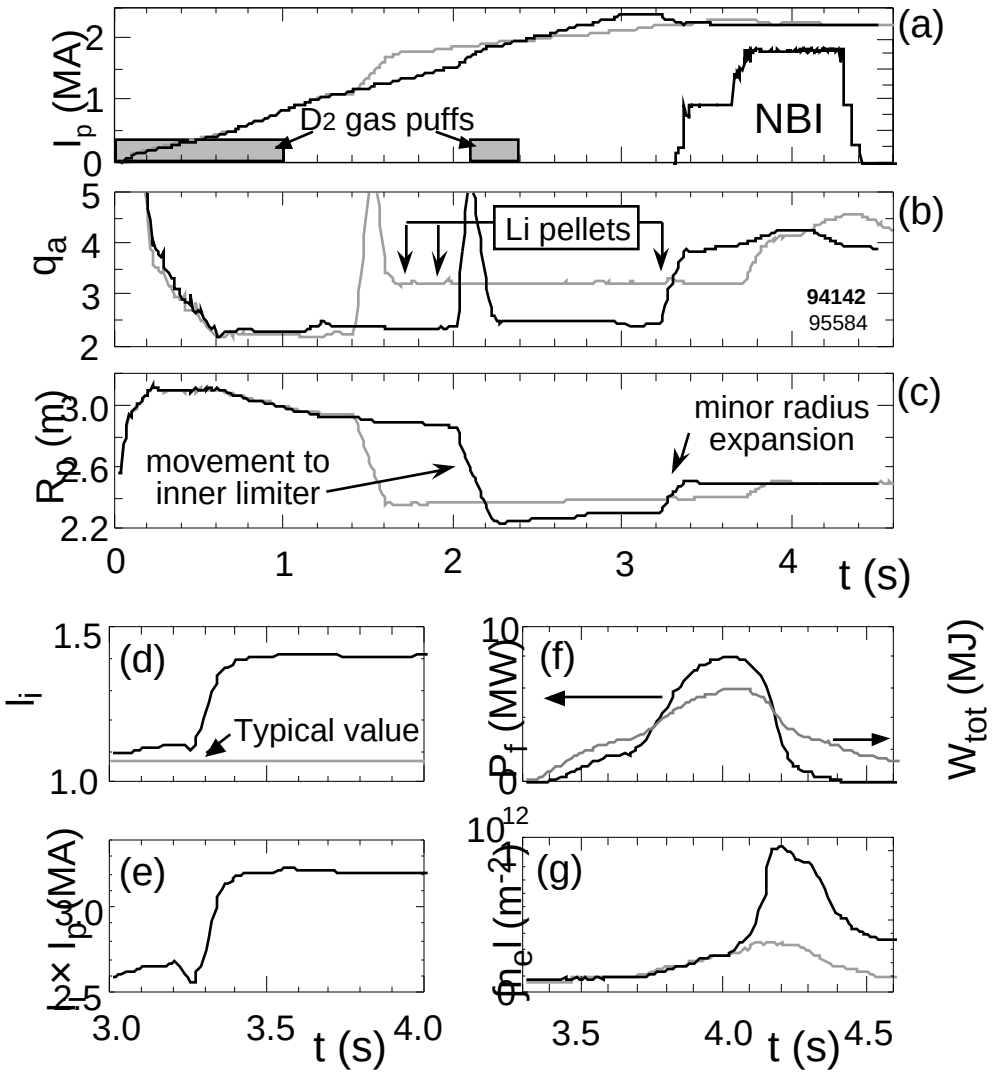

Figure 2 Time evolution of plasma parameters for high l_i *plasmas. Frames (a - c) show plasma current, edge safety factor, and major radius. Frames (d - g) show plasma internal inductance,* $l_i \times I_p$ *product, D-T fusion power and plasma total stored energy, and line integrated edge density. For comparison, frame (g) includes the evolution of an equivalent plasma (dashed trace) in which a density bloom does not occur.*

central electron densities of up to 7×10^{19} m^{-3} and peaking factor $F_{ne} \equiv n_e(0)/\langle n_e \rangle \leq 2.9$ have been reached. Non-inductively driven current of greater than 30% has been computed by TRANSP at I_p = 2 MA with a 27% contribution from the bootstrap current.

The q profile has been measured in plasmas with high l_i using a motional Stark effect (MSE) diagnostic [15]. Compared to plasmas with standard (lower) values of l_i at the same I_p, high l_i I_p plasmas have greater core current density and reduced edge current density. The on-axis safety factor, q_0 varies from 0.75 - 0.8 with an error of 0.04 during the NBI phase.

Unlike TFTR high β_p, high l_i plasmas created by ramping down I_p, the recent discharges did not make a transition to a limiter H-mode. Reducing the edge current density and increasing the edge shear is therefore more effective in reducing the H-mode power threshold than the present techniques used to increase l_i.

III. Beta limit scaling with l_i and pressure peakedness

A general increase in β_N with increasing l_i for TFTR plasmas with monotonic q profiles and I_p > 1 MA is demonstrated in Fig. 3. The maximum β_N for high l_i plasmas at $I_p \geq 2$ MA follow the trend established by plasmas with I_p = 1-2 MA. Pressure profile peaking factors, $F_p \equiv P(0)/\langle P \rangle$ range from 3 - 6.2 in high l_i plasmas. At greater values of F_p, the β_{Nmax} can be reduced substantially. For example, Fig. 3 shows supershot plasmas produced with a lithium conditioned limiter have reached $F_p \sim 8$ and disrupted at low $\beta_N \sim 1.2$.

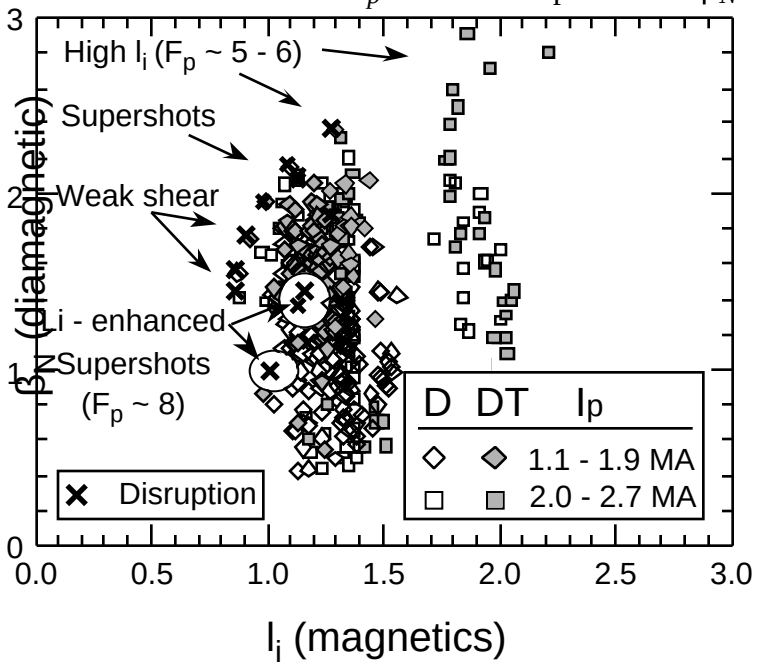

Figure 3 Increase of β_N *as a function of* l_i *for several TFTR plasma operating regimes.*

High l_i plasmas with l_i > 1.3, $I_p \geq 2$ MA and $B_0 \geq 5.1$T and $F_p \sim 5$ have exceeded $\beta_N = 2$ without disruption. These plasmas were limited in performance by density blooms. Only one high l_i plasma has disrupted at high β_N. This disruption, which had $\beta_N = 2.38$, was generated in a high l_i plasma with I_p = 2 MA, B_0 = 4.8 T specifically designed to reach β_{Nmax} before the onset of a bloom. This can be compared to a supershot disruption with I_p = 2.5 MA, B_0 = 5.1 T, equivalent F_p, and β_{Nmax} = 1.85. The ratio of l_i between these plasmas is 1.29 and the ratio of the beta limits also 1.29, consistent with a linear scaling of β_{Nmax} with l_i.

This general behavior of the β limit can be modelled by ideal MHD theory. A study of the instability threshold β_N and $\beta_N^* \equiv 2\mu_0\langle p^2\rangle^{0.5} a/B_0 I_p$, as a function of l_i and F_p for ideal low-n modes ($1 \leq n \leq 4$) using the PEST code is shown in Fig. 4. High-n modes were also tested, but do not set the stability limit for $2.5 \leq F_p \leq 6$. The equilibrium pressure and q profiles, and boundary shapes used for the study are taken from TRANSP runs of experimental discharges which exhibit extreme values of F_p and l_i. The profiles for these actual plasmas are then used to produce phantom equilibria with interpolated, and slightly extrapolated values of the profile peaking parameters. The q_0 has also been scaled to be slightly greater than one in order to eliminate the robust m = 1, n = 1 instability, computed by ideal MHD stability codes for experimentally stable plasmas which are measured to have $q_0 < 1$. The q_a was held constant (4.9) in this study, and no conducting wall was used.

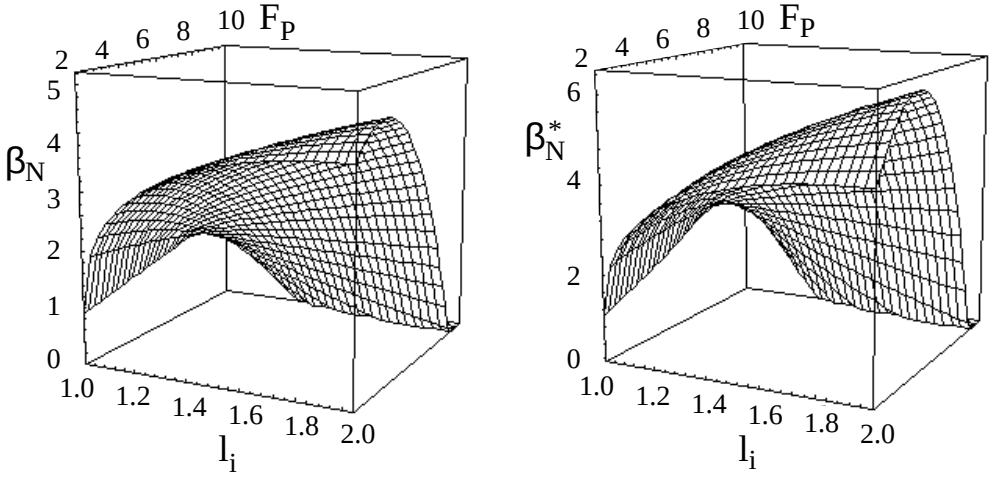

Figure 4 Dependence of stability to ideal low-n modes as a function of l_i *and* F_p.

At sufficiently low l_i, β_{Nmax} decreases rapidly due to a purely current-driven kink mode. The decrease of β_{Nmax} shown at high values of $F_p \sim 8$ and higher l_i is similar to that observed in lithium-enhanced supershots (Fig. 3). A local maximum stable operating value of β_N^* is found as a function of F_p for a given l_i. The maximum l_i that can be reached will either be constrained by technical considerations, or by the occurrence of internal mode destabilization. Therefore, an optimized operating point with a given (l_i, F_p) can be reached. In the range of l_i created in the present experiments, the β_N* is optimized at $F_p \sim 5$. The modelled instability is normally a global kink/ballooning mode.

Experimentally, there is a positive correlation observed between increased F_p and τ_E in supershots and high l_i plasmas. Thus, maximizing β_N* or P_f for a given l_i can occur at greater F_p than the computed optimally stable value when operating at maximum l_i I_p B_0 due to insufficient τ_E. In this case, τ_E may be increased by operating at a higher F_p thereby optimizing against combined stability and τ_E constraints.

Further stability analyses were performed for TRANSP reconstructions of the high l_i experimental plasmas. The q profiles varied depending on the exact low q_a startup technique used. Pressure profiles were varied by considering different discharges with F_p in the range 3.6 - 5.1. In cases using $F_p > 5$, the computed stability limit β_{Nmax} varies from 2.3 - 2.6 consistent with the intentional high l_i disruption at $\beta_{Nmax} = 2.38$ and $F_p = 6.2$ created experimentally. Both low and high-n modes were computed to be unstable. This is above the limit for high $I_p > 2.3$ MA supershot plasmas of $\beta_N \leq 2$. The β_{Nmax} for equilibria with $F_p = 3.6$ varied from 2.8 - 3.3 depending on the q profile considered. Low-n kink/ballooning modes set the limit in this case.

IV. MHD instabilities and impact on confinement

Stationary magnetic perturbations (SMPs) [16] (also referred to as quasi-stationary modes (QSMs) in JET [17] and JT-60U [18]), have occurred at several distinct phases of the high l_i plasma evolution. These modes typically caused disruption during the ohmic phase. During beam heating, performance is limited by a reduction in τ_E due to an increase in particle recycling and edge plasma density that occurs after the onset of the SMP.

In all cases, techniques have been developed to stabilize SMPs. A combination of D_2 gas puffing, plasma initiation on a higher-recycling outer limiter, and a rapid initial decrease of q_a has stabilized the mode during the initial second of the discharge evolution. Additional gas puffing during the transition to the inner limiter has eliminated SMPs during this phase. SMPs have also been observed after the minor radius expansion, perhaps due to eddy currents generated in the vacuum vessel. Plasma rotation, generated by a 200-300 ms initial period of co-injected neutral beams has stabilized the mode, similar to results in JT-60U[18]. Injection of a lithium pellet 50 ms after the expansion has also suppressed the mode. Pellet injection has also been used to suppress SMPs during the decrease of I_p during normal discharge termination.

Low order rational MHD tearing modes, which have been modelled as neoclassical ∇p driven modes in TFTR [19] have been absent from the recent high l_i plasmas, similar to supershots with $I_p > 2$ MA. Fishbones and sawteeth have been observed. The $q = 1$ radius of these plasmas occurs at $r/a = 0.35$, which is larger than the value 0.25 typically observed in supershot plasmas. This result is based on the sawtooth inversion radius as measured by an electron cyclotron emission (ECE) diagnostic. Plasmas with larger $q = 1$ radii do not suffer a reduction in τ_E as long as sawteeth are stabilized during NBI.

Sawtooth stabilization in these plasmas is analyzed in terms of the Zakharov-Rogers two-fluid collisionless m=1 reconnection model [20]. Data points in Fig. 5 represent time points chosen at the half-maximum rise and fall of W_{tot}, at the maximum stored energy, and at maximum critical shear for 20 experimental discharges. The sawtooth period, τ_{saw}, which was determined from electron temperature fluctuations as measured by ECE, increases with the ratio of the critical shear to the TRANSP computed shear, q'_{crit}/q', at the $q = 1$ surface. Experimentally, plasmas are found to be unstable when $q'_{crit}/q'_{|_1} \leq 1$ and stable when $q'_{crit}/q'_{|_1} \geq 2.1$ in agreement with theory. During the initial heating phase of the plasma, the stability criterion is met ($1 \leq q'_{crit}/q'_{|_1} \leq 2.1$) yet sawteeth are typically observed while the pressure gradient builds. The criterion is therefore not strictly applicable during dynamic heating phases.

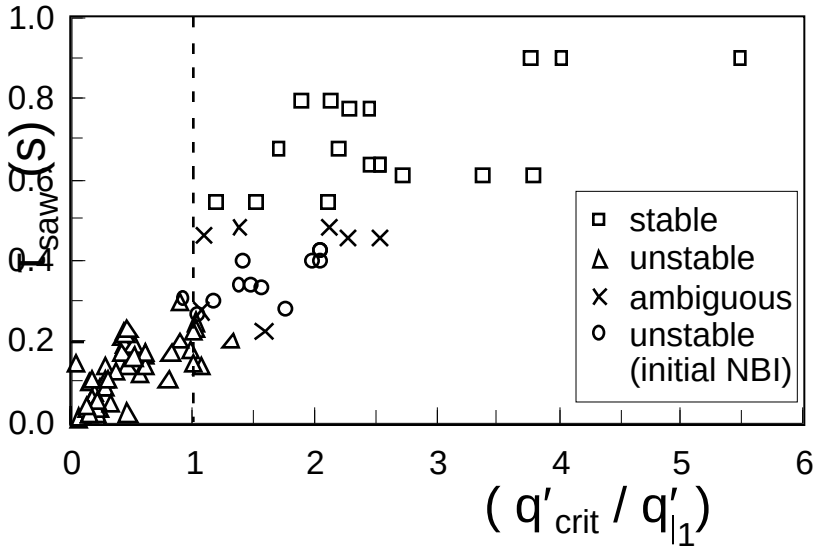

Figure 5 Sawtooth period vs. the ratio of the Zakharov-Rogers critical shear model of sawooth stabilization to the TRANSP computed shear at $q = 1$ *in high* l_i *plasmas. Squares indicate stability; triangles instability. Circles indicate that a sawtooth occurred during the inital phase (*$\Delta t \sim 3\ \tau_E$*) of NBI. Crosses indicate that a crash occured at NBI termination.*

When the modes considered above are stabilized, techniques to raise τ_E in standard supershot plasmas have been used to improve performance. The established technique of lithium conditioning of the limiter has produced τ_E up to 240 ms in D-T plasmas, which slightly exceeds that of supershot plasmas with $P_b > 30$ MW. Also, a positive isotopic mass dependence of τ_E in D-T plasmas has been observed, typically yielding an increase of greater than 20% in high l_i I_p plasmas. Details of the isotope effect in these and other TFTR plasmas can be found in a companion paper by Scott, *et al.* [21].

V. Reversed shear plasmas with increased l_i

Plasmas with reversed shear (RS) and high l_i were created by using NBI during the initial rise of I_p [11], and then rapidly decreasing I_p during NBI. In these plasmas, $\varepsilon\beta_p$ reached 1.1, $\beta_N = 2.6$, and $H \equiv \tau_E/\tau_{E\ ITER-89P} = 3.5$. The measured (using MSE) $q_0 = 3.5 \pm 0.5$ and $q_{min} = 2.5$ - 3. These plasmas are computed to have robust stability to high-*n* modes over 65-80% of the plasma minor radius and access to the second stability region in the core (Fig. 6). The computed low-*n* mode stability limit increases at high l_i compared to standard RS plasmas and agrees with the experimental disruption limit. For example, RS plasmas with $l_i = 0.9$ and $I_p = 1.6$ MA have disrupted at $\beta_N = 1.6$, in agreement with an ideal $n = 1$ mode becoming unstable at this value. The high l_i RS plasmas at $l_i = 1.25$ and $I_p = 0.9$ MA disrupted at $\beta_N = 2.9$, also in agreement with the computed $n = 1$ ideal instability threshold.

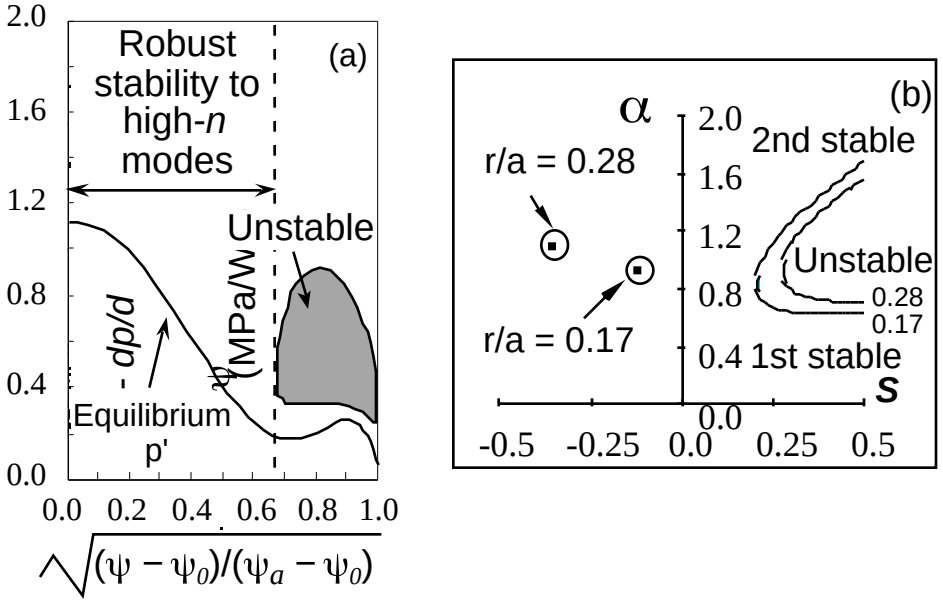

Figure 6 High-n stability for $\varepsilon\beta_p$ *=1 plasma with reversed shear in the plasma core and increased edge shear. Frame (a) shows the equilibrium p' vs. The square root of the normalized poloidal flux, and the unstable region to high-*n *ballooning modes. Frame (b) shows an* (α, S) *diagram for two minor radial positions,* r/a = *0.17 and ,* r/a = *0.28.*

VI. Conclusion

A new technique of low q_a plasma initiation in TFTR has allowed plasmas with increased l_i to be generated at I_p up to 2.3 MA. With sawteeth stabilized, the increased q = 1 radius in these plasmas does not degrade confinement. Rather, the increased l_i I_p product has yielded an increase in $\beta_{N\,max}$. Consequently, peak DT fusion power levels which rival the highest attained in TFTR have been generated. At the highest values of l_i I_p B_0, performance in these plasmas is no longer limited by stability, but by a reduction in τ_E caused by large density blooms generated by the increased power load to the limiter. Future experiments including a radiative mantle of krypton are planned to eliminate this constraint. High l_i plasmas with reversed shear in the core have also been created, and have demonstrated an increase in $\beta_{N\,max}$ as l_i is increased by increasing the edge magnetic shear.

---

[1] McGUIRE, K. M., ADLER, H., ALLING, P., et al., Phys. Plasmas **2** (1995) 2176.

[2] TAYLOR, T. et al., Workshop on Tokamak Concept Improvement, Varenna, Italy, 1994, Editrice Compositori, Bologna, **1** (1995) 111.

[3] FERRON, J. R., et al., Phys. Fluids B **5** (1993) 2532.

[4] LAO, L. L., et al., Phys. Rev. Lett. **70** (1993) 3435.

[5] KAMADA, Y., USHIGUSA, K., NEYATANI, Y., et al., Plasma Phys. Contr. Nucl. Fus. Res. 1994, IAEA, Vienna, **1** (1995) 651.

[6] SABBAGH, S. A., et al., Phys. Fluids B **3** (1991) 2277.

[7] MAUEL, M. E., NAVRATIL, G.A., SABBAGH, S. A., et al., Plasma Phys. Contr. Nucl. Fus. Res. 1992, IAEA, Vienna, **1** (1993) 205.

[8] HOWL, W., TURNBULL, A., TAYLOR, T., et al., Phys. Fluids B **4** (1992) 1724.

[9] BELL, M. G., BARNES, C.W., BUDNY, R.V., et al., Plasma Phys. Contr. Nucl. Fus. Res. 1994, IAEA, Vienna, **1** (1995) 171.

[10] SABBAGH, S. A., NAVRATIL, G. A., MAUEL, M. E., et al., Plasma Phys. Contr. Nucl. Fus. Res. 1994, IAEA, Vienna, **1** (1995) 663.

[11] LEVINTON, F. M., et al., Phys. Rev. Lett. **75** (1995) 4417.

[12] NAZIKIAN, R., et al., paper F1-CN-64/A2-4 this conference.

[13] FREDRICKSON, E.D., et al., in preparation for submission to Nuclear Fusion Letters.

[14] MANSFIELD, D.K., et al., Phys. Plasmas **3** (1996) 1892.

[15] LEVINTON, F .M., et al., Phys. Rev. Lett. **63** (1989) 2060.

[16] TAKAHASHI, H., et al., "Interpretability of magnetic diagnostics in tokamaks - Search for a locked mode in TFTR", 7th Intl. Conference on Plas. Phys. and Control. Nucl. Fus. (1995) Toki-city, Japan.

[17] SNIPES, J. A., et al., Nucl. Fusion **28** (1988) 1085.

[18] YOSHINO, R., NEYATANI, Y., ISEI, N., et al., Plasma Phys. Contr. Nucl. Fus. Res. 1994, IAEA, Vienna, **1** (1995) 685.

[19] CHANG, Z., et al., Phys. Rev. Lett. **74** (1995) 4663.

[20] ZAKHAROV, L. and ROGERS, B., Phys. Fluids B **4** (1992) 3285.

[21] SCOTT, S., et al. paper F1-CN-64/A6-6 , this conference.